

Recent J/ψ Results from BESII

Xiaoyan SHEN (for the BES Collaboration)

*Institute of High Energy Physics, Chinese Academy of Science,
Beijing 100049, People's Republic of China*

The studies on the multi-quark candidates, light scalar mesons and excited baryon states at BES are presented, based on 5.8×10^7 J/ψ data collected with BESII detector. The measurements of some J/ψ and η_c decays are presented too. We also report the searches for the lepton flavor violation and pentaquark states in J/ψ decays.

Keywords: multiquark state; J/ψ decay; scalar meson, branching ratio; baryon

1. Introduction

BES, as described in ref. ¹, is a large general purpose solenoidal detector at the Beijing Electron Positron Collider (BEPC). Since 1998, the BES detector has been upgraded to BESII. The 5.8×10^7 J/ψ events have been accumulated with BESII since then, which provides a good laboratory for the study of the non- $q\bar{q}$ states and hadron spectroscopy.

2. Study of the multiquark candidates

2.1. Near $p\bar{p}$ threshold enhancement in $J/\psi \rightarrow \gamma p\bar{p}$

There is an accumulation of evidence for anomalous behavior in the $p\bar{p}$ system near $2m_p$ mass threshold. We analyze $J/\psi \rightarrow \gamma p\bar{p}$ with BESII J/ψ data ². Fig. 1 shows the $p\bar{p}$ invariant mass distribution for selected events. Except for a peak near $M_{p\bar{p}} = 2.98$ GeV/c^2 that is consistent in mass, width, and yield with expectations for $J/\psi \rightarrow \gamma\eta_c$, $\eta_c \rightarrow p\bar{p}$ ³ and a broad enhancement around $M_{p\bar{p}} \sim 2.2$ GeV/c^2 , there is a narrow, low-mass peak near the $p\bar{p}$ mass threshold.

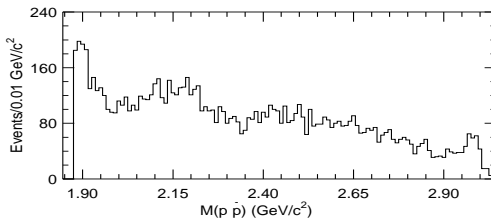


Fig. 1. The $p\bar{p}$ invariant mass distribution in $J/\psi \rightarrow \gamma p\bar{p}$ decays.

The low mass region of the $p\bar{\Lambda}$ distribution is fitted by an acceptance-weighted S -wave Breit-Wigner (BW) function and $f_{\text{bkg}}(\delta)$ which represent the low-mass enhancement and the background, respectively. The fit yields 928 ± 57 events in the BW function with a peak mass of $M = 1859_{-10}^{+3} {}^{+5}_{-25} \text{ MeV}/c^2$ and a full width of $\Gamma < 30 \text{ MeV}/c^2$ at a 90% confidence level (CL).

2.2. The anomalous enhancements near the $m_p + M_{\bar{\Lambda}}$ and $m_K + M_{\bar{\Lambda}}$ mass thresholds in $J/\psi \rightarrow pK^-\bar{\Lambda} + c.c.$ decays

The decay of $J/\psi \rightarrow pK^-\bar{\Lambda} + c.c$ are studied ⁴. Fig. 2 (left) shows the $p\bar{\Lambda}$ invariant mass spectrum for the selected events, where an enhancement is evident near the mass threshold. The $pK^-\bar{\Lambda}$ Dalitz plot is shown in Fig. 2 (right). In addition to bands for the well established $\Lambda^*(1520)$ and $\Lambda^*(1690)$, there is a significant N^* band near the $K^-\bar{\Lambda}$ mass threshold, and a $p\bar{\Lambda}$ mass enhancement in the right-upper part of the Dalitz plot, isolated from the Λ^* and N^* bands.

This enhancement can be fitted with an acceptance weighted S -wave Breit-Wigner together with a function $f_{PS}(\delta)$ describing the phase space contribution. The fit gives a peak mass of $m = 2075 \pm 12 \text{ MeV}$, a width $\Gamma = 90 \pm 35 \text{ MeV}$ and a branching ratio

$$BR(J/\psi \rightarrow K^- X)BR(X \rightarrow p\bar{\Lambda}) = (5.9 \pm 1.4) \times 10^{-5}.$$

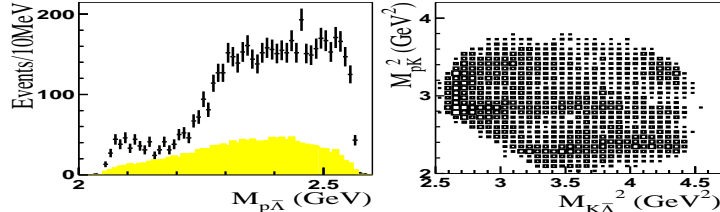


Fig. 2. Left: the points with error bars indicate the measured $p\bar{\Lambda}$ mass spectrum; the shaded histogram indicates phase space MC events (arbitrary normalization). Right: the Dalitz plot for the selected event sample.

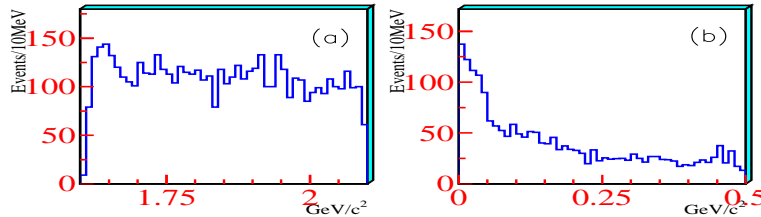


Fig. 3. (a). The $m_{K^-\bar{\Lambda}}$ invariant mass spectrum from $J/\psi \rightarrow pK^-\bar{\Lambda}$. (b). The $m_{K^-\bar{\Lambda}} - m_K - m_{\bar{\Lambda}}$ distribution after the efficiency and phase space correction.

As mentioned above, the $pK^-\bar{\Lambda}$ Dalitz plot, Fig. 2 (right), shows a significant N^* band near the $K^-\bar{\Lambda}$ mass threshold. This band corresponds to an enhancement

near the $K^-\bar{\Lambda}$ mass threshold in the one dimension projection of $m_{K^-\bar{\Lambda}}$, shown in Fig. 3(a). The $m_{K^-\bar{\Lambda}} - m_{K^-} - m_{\bar{\Lambda}}$ distribution, Fig. 3(b), after the efficiency and phase space correction presents a more obvious peak at the $K^-\bar{\Lambda}$ mass threshold.

The partial wave analysis results show that the mass and width of this enhancement, N_x , are around 1500 - 1650 MeV and 70 - 110 MeV, respectively, the J^P favors $1/2^-$ and the product branching ratio $Br(J/\psi \rightarrow p\bar{N}_x) \times Br(\bar{N}_x \rightarrow K^-\bar{\Lambda})$ is around 2×10^{-4} . The big product branching ratio indicates a large coupling of N_x to $K\Lambda$.

3. Light scalar mesons

3.1. The σ and κ

There have been hot debates on the existence of σ and κ . The decay of $J/\psi \rightarrow \omega\pi^+\pi^-$, with the ω decaying to $\pi^+\pi^-\pi^0$, is studied for σ ⁵.

Fig. 4 (left) shows the $\pi^+\pi^-$ invariant mass spectrum recoiling against the ω for the selected $J/\psi \rightarrow \omega\pi^+\pi^-$ events. The Dalitz plot of this channel is shown in Fig. 4 (right). At low $\pi\pi$ masses, a broad enhancement which is due to the σ pole is clearly seen. This peak is evident as a strong band along the upper right-hand edge of the Dalitz plot.

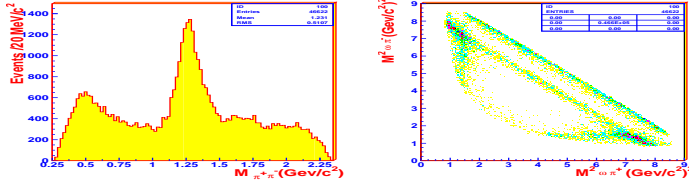


Fig. 4. Left: distribution of $\pi^+\pi^-\pi^0$ mass. Right: Dalitz plot.

Two independent Partial wave analyses (PWA) have been performed on this channel. Different analysis methods and four parametrizations of the σ amplitude give consistent results for the σ pole. The average σ pole position is determined to be $(541 \pm 39) - i(252 \pm 42)$ MeV.

The κ is studied from $J/\psi \rightarrow \bar{K}^*(892)K^+\pi^-$ and $K^+K^-\pi^+\pi^-$ decays through partial wave analysis. Three independent analyses have been performed and different parametrizations of κ pole are used. The preliminary results show the evidence of κ near the $K\pi$ threshold. Its pole position is around $(760 \sim 840) - i(310 \sim 420)$ MeV.

3.2. $J/\psi \rightarrow \omega K^+K^-$

Fig. 5 shows the K^+K^- invariant mass distribution from $J/\psi \rightarrow \omega K^+K^-$. The crosses are data and the shaded area indicates background events from the ω side-band estimation. A dominant feature of this channel is the structure around 1.74 GeV, denoted as $f_0(1710)$. A partial wave analysis (PWA) shows that the J^P of

this structure favors 0^+ and the mass and width are optimized at $M = 1738 \pm 30$ MeV, $\Gamma = 125 \pm 20$ MeV.

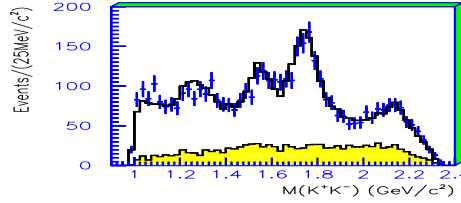


Fig. 5. The K^+K^- invariant mass distribution from $J/\psi \rightarrow \omega K^+K^-$ (crosses). The full histogram shows the maximum likelihood fit and the shaded histogram the background estimated from ω sidebands.

In $J/\psi \rightarrow \omega\pi^+\pi^-$ ⁵, there is no definite evidence for the presence of $f_0(1710)$. Therefore, we find at the 95% confidence level

$$\frac{BR(f_0(1710) \rightarrow \pi\pi)}{BR(f_0(1710) \rightarrow K\bar{K})} < 0.11.$$

3.3. $J/\psi \rightarrow \phi\pi^+\pi^-$ and $J/\psi \rightarrow \phi K^+K^-$ (preliminary)

Fig. 6 (a) and (b) show the $\pi^+\pi^-$ and K^+K^- invariant mass distributions from $J/\psi \rightarrow \phi\pi^+\pi^-$ and ϕK^+K^- , respectively. The shaded histograms correspond to the backgrounds estimated from ϕ sidebands.

The $\phi\pi^+\pi^-$ and ϕK^+K^- data are fitted simultaneously by using partial wave analysis, constraining resonance masses and widths to be the same in both sets of data. The full histograms in Fig. 6 (left) and (right) show the maximum likelihood fit.

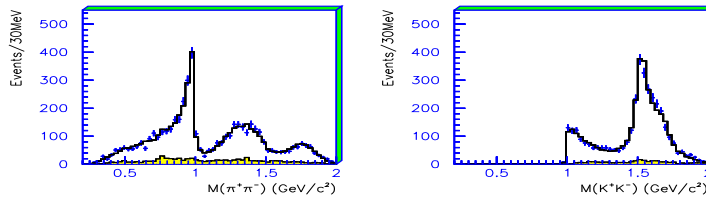


Fig. 6. Left: the mass spectrum of $\pi^+\pi^-$ in $J/\psi \rightarrow \phi\pi^+\pi^-$. Right: the mass spectrum of K^+K^- in $J/\psi \rightarrow \phi K^+K^-$. Crosses are data and histograms are PWA fit projections.

The $f_0(980)$ is observed clearly in both sets of data. The Flatté form:

$$f = \frac{1}{M^2 - s - i(g_1\rho_{\pi\pi} + g_2\rho_{K\bar{K}})}.$$

has been used to fit the $f_0(980)$ amplitude. Here ρ is Lorentz invariant phase space, $2k/\sqrt{s}$, k refers to π or K momentum in the rest frame of the resonance. The present

data offer the opportunity to determine the parameters of $f_0(980)$ accurately: $M = 965 \pm 8(sta) \pm 6(sys)$ MeV, $g_1 = 165 \pm 10(sta) \pm 15(sys)$ MeV, $g_2/g_1 = 4.21 \pm 0.25(sta) \pm 0.21(sys)$.

The $\phi\pi\pi$ data also exhibit a strong peak centered at $M = 1335$ MeV. It may be fitted with $f_2(1270)$ and a dominant 0^+ signal made from $f_0(1370)$ interfering with a smaller $f_0(1500)$ component. The Mass and width of $f_0(1370)$ are determined to be: $M = 1350 \pm 50$ MeV and $\Gamma = 265 \pm 40$ MeV.

There is also a signal at around 1.79 GeV in $J/\psi \rightarrow \phi\pi^+\pi^-$ with $M = 1790^{+40}_{-30}$ MeV and $\Gamma = 270^{+60}_{-30}$ MeV. The spin 0 is preferred over spin 2.

3.4. $J/\psi \rightarrow \gamma\pi\pi$ (preliminary)

The $\pi^+\pi^-$ and $\pi^0\pi^0$ invariant mass distributions from $J/\psi \rightarrow \gamma\pi^+\pi^-$ and $\gamma\pi^0\pi^0$ are shown in Fig. 7 (left) and (right). The partial wave analyses are carried out in the 1.0-2.3 GeV $\pi\pi$ mass range. Two 0^{++} states exist in the mass lower than 1.8 GeV. The first one peaks at $1466 \pm 6 \pm 16$ MeV with a width of $108^{+14}_{-11} \pm 21$ MeV, which is approximately consistent with $f_0(1500)$. Due to the large interference between S-wave states, a possible contribution from $f_0(1370)$ cannot be excluded. The second 0^{++} peaks at around 1.75 GeV. If it is the same state with that observed in $J/\psi \rightarrow \gamma K\bar{K}$ ⁶, we obtain the ratio of decaying to $\pi\pi$ and $K\bar{K}$ as $0.41^{+0.08}_{-0.15}$.

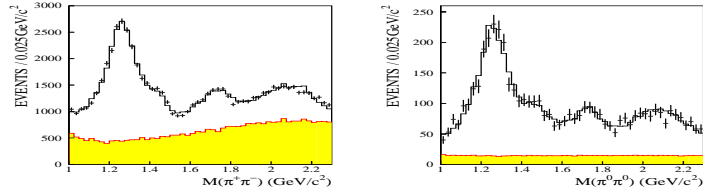
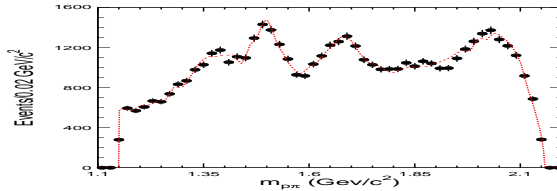


Fig. 7. Left: the mass spectrum of $\pi^+\pi^-$ in $J/\psi \rightarrow \gamma\pi^+\pi^-$. Right: the mass spectrum of $\pi^0\pi^0$ in $J/\psi \rightarrow \gamma\pi^0\pi^0$. Crosses are data and histograms are PWA fit projections.

4. Study of the excited baryon states from $J/\psi \rightarrow p\bar{n}\pi^- + c.c$

The πN system in decays of $J/\psi \rightarrow \bar{N}N\pi$ is limited to be isospin 1/2 by isospin conservation. This provides a big advantage in studying $N^* \rightarrow \pi N$ compared with πN and γN experiments which mix isospin 1/2 and 3/2 for the πN system. Fig. 8 shows the πN invariant mass spectrum from $J/\psi \rightarrow p\bar{n}\pi^-$. Besides two well known N^* peaks at 1500 MeV and 1670 MeV, there are two new, clear N^* peaks in the $p\pi$ invariant mass spectrum around 1360 MeV and 2030 MeV. They are the first direct observation of the $N^*(1440)$ peak and a long-sought ‘missing’ N^* peak above 2 GeV in the πN invariant mass spectrum. A simple Breit-Wigner fit gives the mass and width for the $N^*(1440)$ peak as $1358 \pm 6 \pm 16$ MeV and $179 \pm 26 \pm 50$ MeV, and for the new N^* peak above 2 GeV as $2068 \pm 3^{+15}_{-40}$ MeV and $165 \pm 14 \pm 40$ MeV, respectively.

Fig. 8. *The invariant mass spectrum of πN*

5. Other Results

The mass, width of η_c , as well as some of its decay branching ratios are measured with BESII 5.8×10^7 J/ψ events. The $J/\psi \rightarrow \gamma f_2(1270)f_2(1270)$ decay is first observed and measured. We also present much improved measurements on $J/\psi \rightarrow \pi^+\pi^-\pi^0$ ⁷, $K_s K_L$ ⁸ and $p\bar{p}$ ⁹ decays.

The lepton flavor violation (LFV) is searched for from $J/\psi \rightarrow e\mu$, $\mu\tau$ and $e\tau$ decays, the LFV processes. The observed signal events are consistent with the background level. The upper limits of the decay branching fractions are set¹⁰.

We also search for the pentaquark state $\Theta(1540)$ in $J/\psi \rightarrow K_S^0 p K^- \bar{n}$ and $K_S^0 \bar{p} K^+ n$ final states with K_S^0 decaying to $\pi^+\pi^-$. No clear Θ signal is observed. The upper limits are set¹¹.

Acknowledgments

We acknowledge the staff of the BEPC and IHEP computing center for their hard efforts. This work is supported in part by the National Natural Science Foundation of China under contracts Nos. 19991480, 10225524, 10225525, 10175060 (USTC), and No. 10225522 (Tsinghua University), the Chinese Academy of Sciences under contract No. KJ 95T-03, the 100 Talents Program of CAS under Contract Nos. U-11, U-24, U-25, and the Knowledge Innovation Project of CAS under Contract Nos. U-602, U-34 (IHEP); and by the Department of Energy under Contract No. DE-FG03-94ER40833 (U Hawaii)

References

1. BES Collaboration, Nucl. Instr. Meth., **A344** 319 (1994), **A458** 627 (2001).
2. BES Collaboration, Phys. Rev. Lett., 91 (2003) 022001
3. BES Collaboration, Phys. Lett. **B555**, (2003) 174 and **B578**, (2004) 16
4. BES Collaboration, Phys. Rev. Lett., 93 (2004) 112002
5. BES Collaboration, Phys. Lett. **B598**, (2004) 149
6. BES Collaboration, Phys. Rev. **D68**, (2003) 052003
7. BES Collaboration, Phys. Rev. **D70**, (2004) 012005
8. BES Collaboration, Phys. Rev. **D69**, (2004) 012003
9. BES Collaboration, Phys. Lett. **B591**, (2004) 42
10. BES Collaboration, Phys. Lett. **B561**, (2003) 49, **B598**, (2004) 172
11. BES Collaboration, Phys. Rev. **D70**, (2004) 012004